Title
INFLUENCE OF MICROSTRUCTURE ON NEAR-THRESHOLD FATIGUE CRACK PROPAGATION IN ULTRA-HIGH STRENGTH STEEL

Author
Ritchie, Robert O.

Publication Date
1976-11-01

To be presented at the Metals Society
Conference "FATIGUE 1977",
Cambridge, England, March 28 - 30, 1977

LBL-5730
c.1

INFLUENCE OF MICROSTRUCTURE ON NEAR-THRESHOLD FATIGUE CRACK PROPAGATION IN ULTRA-HIGH STRENGTH STEEL

Robert O. Ritchie

November 1976

Prepared for the U. S. Energy Research and
Development Administration under Contract W-7405-ENG-48

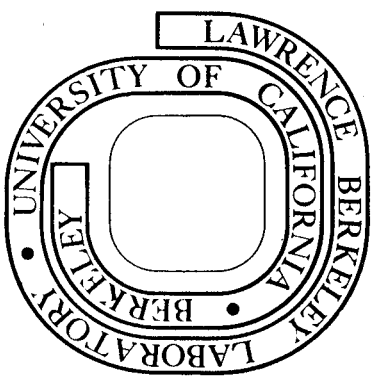

LBL-5730
c.1

DISCLAIMER

Invited Paper for The Metals Society
Conference, FATIGUE 1977; Cambridge,
United Kingdom, March, 1977.

LBL-5730

INFLUENCE OF MICROSTRUCTURE ON NEAR-THRESHOLD FATIGUE CRACK PROPAGATION IN ULTRA-HIGH STRENGTH STEEL

Robert O. Ritchie*

Materials and Molecular Research Division, Lawrence Berkeley Laboratory
and Department of Materials Science and Engineering,
University of California, Berkeley, California 94720

ABSTRACT

Fatigue crack propagation behaviour of an ultra-high strength, silicon-modified AISI 4340 alloy steel (300-M) has been investigated in moist air over an extremely wide range of growth rates from 10^{-8} to 10^{-1} mm/cycle (10^{-9} - 10^{-3} in/cycle). Particular emphasis has been devoted to the influence of microstructure on fatigue fracture behaviour near the threshold stress intensity, ΔK_o, below which crack growth cannot be detected. By varying microstructure through quench and tempering and isothermal transformations, the threshold stress intensity and near-threshold crack propagation rates are observed to be influenced by mean stress (load ratio), material strength, grain size and impurity segregation. The threshold ΔK_o for crack propagation is found to be inversely related to the strength of the steel, and a relationship between ΔK_o and cyclic yield stress is observed. It is shown how near-threshold crack growth resistance can be improved by i) cyclic softening, ii) coarsening the prior austenite grain size and iii) controlling impurity segregating to grain boundaries. These

---

*At present, at the Department of Mechanical Engineering, Massachusetts Institute of Technology, Cambridge, Massachusetts 02139.

effects are contrasted with crack propagation behaviour at higher growth rates. A semi-quantitative model is developed to rationalise near-threshold fatigue crack growth behaviour, based on the environmental influence of hydrogen, evolved from crack tip surface reactions with water vapour in moist air.

Influence of Microstructure on Near-Threshold Fatigue Crack Propagation in Ultra-High Strength Steel, Robert O. Ritchie, Massachusetts Institute of Technology

Synopsis

Fatigue crack propagation behaviour of an ultra-high strength, silicon-modified AISI 4340 alloy steel (300-M) has been investigated in moist air over an extremely wide range of growth rates from 10^{-8} to 10^{-1} mm/cycle (10^{-9} - 10^{-3} in/cycle). Particular emphasis has been devoted to the influence of microstructure on fatigue fracture behaviour near the threshold stress intensity, ΔK_o below which crack growth cannot be detected. By varying microstructure through quench and tempering and isothermal transformations, the threshold stress intensity and near-threshold crack propagation rates are observed to be influenced by mean stress (load ratio), material strength, grain size and impurity segregation. The threshold ΔK_o for crack propagation is found to be inversely related to the strength of the steel, and a relationship between ΔK_o and cyclic yield stress is observed. It is shown how near-threshold crack growth resistance can be improved by i) cyclic softening, ii) coarsening the prior austenite grain size and iii) controlling impurity segregation to grain boundaries. These effects are contrasted with crack propagation behaviour at higher growth rates. A semi-quantitative model is developed to rationalise near-threshold fatigue crack growth behaviour, based on the environmental influence of hydrogen, evolved from crack tip surface reactions with water vapour in moist air.

Introduction

In many engineering applications where design against cyclic loading is a prime consideration, the principal factor controlling the lifetime of a particular component is often the rate at which fatigue cracks can grow from pre-existing defects. Accordingly, over the past 10 to 15 years, a large volume of data has been generated on fatigue crack propagation behaviour at growth rates in excess of 10^{-6} mm/cycle. Although this information is useful for most structural engineering applications (determining safe inspection intervals in aircraft, for example), in situations where structural and machinery components are subject to extreme high frequency, low amplitude loadings for 10^{10} to 10^{12} cycles, a need exists for an assessment of fatigue crack propagation behaviour at growth rates below 10^{-6} mm/cycle. This area has received comparatively little attention in the literature, and consequently there is both little understanding of the growth mechanisms at very low propagation rates and a substantial lack of reliable engineering data. Such information, particularly a knowledge of a threshold stress intensity below which cracks cannot propagate, has been shown to be essential in the analysis of such problems as cracking in turbine rotor shafts[1] and acoustic fatigue of welds in gas ducts in magnox reactors.[1,2]

The application of linear elastic fracture mechanics and related small scale crack tip plasticity has provided the basis for describing the phenomenon of fatigue crack propagation.[3] Many investigators have confirmed that the crack growth rate per cycle (da/dN) is primarily controlled by the alternating stress intensity (ΔK), through an expression[4] of the form:

$$\frac{da}{dN} = C\,\Delta K^m , \qquad \ldots(1)$$

where 'C' and 'm' are scaling constants, and ΔK is given by the difference between the maximum and minimum stress intensities for each cycle, ie. $\Delta K = K_{max} - K_{min}$. This expression adequately describes behaviour for the mid-range of growth rates, typically 10^{-5} - 10^{-3} mm/cycle, and can be used here with confidence to predict propagation rates in service components to provide a rational basis for design against failure by fatigue. At higher growth rates, however, when K_{max} approaches K_{Ic}, the fracture toughness, Eq. (1) often underestimates the propagation rate, whereas at lower growth rates it is found to be conservative as ΔK approaches a threshold stress intensity ΔK_o, below which crack propagation cannot be detected.[5-21]

Recent studies have shown that this sigmoidal variation of growth rate with ΔK can be characterised in terms of different primary fracture mechanisms (Fig. 1). For

the mid-range of growth rates (regime B), failure generally occurs in steels by a transgranular ductile striation mechanism[22,23] and there is little influence of microstructure and mean stress (characterised by the load ratio, $R = K_{min}/K_{max}$) on crack growth.[24-26] At higher growth rates (regime C), when K_{max} approaches K_{Ic}, the fracture toughness, growth rates become extremely sensitive to both microstructure and mean stress, due to a departure from striation growth to include static fracture modes, such as cleavage, intergranular and fibrous fracture.[24-26] At low (near-threshold) growth rates (regime A), there is similarly a strong influence of microstructure[12,14,15,17,18] and mean stress[7-11,13-21] on growth rates, together with an increased sensitivity to stress history[6] and environmental effects.[14-16,19,27] Explanations for this behaviour, however, remain a subject of some controversy, involving conflicting views based on crack closure[9-11] and environmental factors.[14-16] Paris and co-workers,[9-11,13] for example, have suggested that the mean stress dependence on ΔK_o and near-threshold growth rates is a direct result of crack closure, ie. contact of the crack surfaces due to residual tensile strains above the minimum load of the fatigue cycle.[28] This was originally proposed without experimental verification,[9-11] although, in a later study,[13] closure was detected using *surface* strain gauge measurements. However, there is now evidence to show that closure may only be significant in surface (plane stress) regions,[29,30] and furthermore is reduced by the presence of an environment[31-33] (as opposed to vacuum) and at low stress intensities.[34] Since threshold measurements involve low stress intensities, where plane strain conditions almost invariably exist, it is unlikely that crack closure can provide a useful explanation for the effect of mean stress on near-threshold growth rates. The influence of the environment on crack growth constitutes an alternative explanation, based on results which show i) slower propagation rates and higher threshold values measured *in vacuo* compared to air,[14-16,19,27] and ii) little or no effect of mean stress for tests *in vacuo*.[15,16] In a later section of this paper we will examine how this can be modelled for near-threshold fatigue crack growth in ultra-high strength steels to encompass both microstructure and mean stress effects. Growth mechanisms in this region have been termed "microstructurally-sensitive",[14-16] but it is still not clear which microstructures provide the best resistance to near-threshold growth. From limited data in the literature, it is probable that material strength and the scale of the microstructure are important variables. Higher threshold values have been observed in lower strength steels by decreasing the yield strength,[12,17] and lower near-threshold growth rates measured in the same steels[17] and titanium alloys[14] by increasing the grain size.

The present paper summarises the results of an investigation to characterise microstructural influences on near-threshold fatigue crack propagation in an ultra-high strength steel, 300-M (composition shown in Table 1). Experiments were designed to systematically examine effects of strength,[18] grain size,[20] and impurity segregation,[21] in the hope that the results may provide some basis for the design of alloys more resistant to very high cycle fatigue failure.

Experimental Measurement of Near-Threshold Growth

Ideally, the threshold stress intensity, ΔK_o, represents the stress intensity where the growth rate is infinitely small, although, for practical measurements proposes, it is more useful to define ΔK_o in terms of a maximum growth rate, calculated from the accuracy of the crack monitoring technique and the number of cycles imposed.[16] In the present investigation, crack lengths were continuously measured using the electrical potential technique,[35] and the threshold ΔK_o was computed from the highest stress intensity at which no growth occurred within 10^7 cycles. Since the crack monitoring technique is at least accurate to 0.1 mm, this corresponds to a maximum growth rate of 10^{-8} mm/cycle (4×10^{-10} in/cycle). To minimize residual stress effects, thresholds were approached using a successive load reduction followed by crack growth procedure. Measurements of crack growth rate were taken, at each load level, over increments of 1-1.5 mm., after which the load was reduced, by less than 10%, and the same procedure followed. The increments, over which measurements of growth rate were taken, represent distances exceeding 100 to 1000 times the maximum plastic zone size generated at the previous (higher) load level, and so any initial retardation in growth rate caused by change in load was negligible. Following ΔK_o measurement, the load was increased in steps and a similar procedure adopted. Higher growth rate tests were performed under continuous constant cyclic loading to yield an extremely wide range of propagation rate data from 10^{-8} to 10^{-1} mm/cycle. Tests were conducted at a cyclic frequency of 50 Hz,

under plane strain conditions, in a controlled atmosphere of humid air at constant temperature (23°C) and constant relative humidity (45%). Full experimental details are given elsewhere.[18,21]

Results

i) Effect of Material Strength

To assess the influence of strength at constant grain size, 1-T compact tension specimens (12.7 mm thick) were oil quenched from 870°C to yield a prior austenite grain size of 20 μm, and tempered for 1 hr at 100, 300, 470 and 650°C. These treatments are hereafter referred to as T100, T300, T470 and T650, respectively. Further specimens were austenitized at 870°C, isothermally held at 250°C (20 deg. C below M_S) and tempered at 300°C to produce a structure (referred to as IS0250) with identical monotonic yield strength to the T100 and T470 conditions. The IS0250 structure was selected in view of its high retained austenite content (12%), which is known to change hardening and stress corrosion cracking characteristics.[18] Ambient temperature mechanical properties of the structures are included in Table 2, and fatigue crack propagation results in Figs. 2-4. It is apparent from these plots that the influence of microstructure and load ratio R is maximized at low and high stress intensities (ie. in regimes A and C of Fig. 1).

For the mid-range of growth rates, represented by the linear portion (regime B) of the growth rate curves, there is little variation in propagation rate between different microstructures at both load ratios. Growth rate curves tend towards a common line of slope (ie. exponent 'm' in Eq. 1) of 2.5 at R=0.05 and 2.7 at R=0.70. Transgranular ductile striation growth (Fig. 5a) was observed to be the mechanism of failure for all structures in this range, consistant with a lack of microstructural and load ratio sensitivity on growth rate behaviour.[24-26] Considering the wide variation of tensile strength (2-fold) and toughness (6-fold) shown by the structures tested, fatigue crack growth in regime B appears independent of such mechanical properties.

At higher stress intensities, growth rate curves display an acceleration in propagation rate as K_{max} approaches K_{Ic} (regime C). Marked effects of microstructure and load ratio can now be seen (Figs. 2-4), with resistance to crack growth decreasing as the toughness is reduced. Fractography of failures in this region confirmed the presence of static modes, as shown in Fig. 5. Areas of microvoid coalescence were present in all structures (eg. Fig. 5b and c), with additional intergranular cracking in the T470 condition, and intergranular and cleavage cracking in T100 (Fig. 5b).

The largest influence of microstructure and load ratio can be seen at low stress intensities in regime A, where growth rates are less than 10^{-6} mm/cycle. Close to the threshold ΔK_o, measured propagation rates become less than a lattice spacing per cycle, indicating that crack growth is not occurring uniformly over the entire crack front. Considering first results for quenched and tempered material at R=0.05 (Fig. 2), it is apparent that tempering temperature exerts a strong influence on threshold values and on near-threshold crack propagation rates. At ΔK = 9 MPa$\sqrt{m}$, for example, the growth rate in the T100 condition is over two orders of magnitude greater than in the T650 condition. As the tempering temperature is raised, the threshold ΔK_o increases from 3.0 to 8.5 MPa$\sqrt{m}$, concurrent with a two-fold reduction in tensile strength. At R=0.70 (Fig. 3), the same trend of increasing ΔK_o with decreased strength is still apparent but the effect is drastically reduced: ΔK_o increases from 2.3 to 3.7 MPa$\sqrt{m}$ for the same reduction in strength. The variations of threshold ΔK_o with monotonic yield strength and ultimate tensile strength (U.T.S.) are plotted in Figs. 6 and 7, respectively, indicating a general trend of an inverse dependence of ΔK_o on material strength. However, far better correlation with ΔK_o is obtained using U.T.S. rather than yield stress. This suggests that strain hardening may be important. The flow stresses within the cyclic plastic zone generated ahead of a growing fatigue crack, however, are governed by cyclic rather than monotonic strain hardening effects. Accordingly, cyclic stress-strain tests were performed to assess cyclic yield strengths; a comparison of cyclic and monotonic stress-strain curves is shown in Fig. 8. All structures can be seen to cyclically soften with the exception of the T100 condition which cyclically hardens, and the IS0250 condition which shows

neither significant hardening nor softening.* Utilising these data, a better correlation can be obtained between threshold ΔK_o and material strength (now plotted as the 0.2% offset cyclic yield stress) as shown in Fig. 9. As cyclic strength is increased, either because of high initial monotonic strength or by cyclic hardening, the threshold for fatigue crack propagation is reduced, to a limiting value of ΔK_o = 3 MPa$\sqrt{m}$ at a yield of 1600 MPa for R=0.05, and 2.3 MPa$\sqrt{m}$ at a yield of 1200 MPa at R=0.70. At greater yield strengths, no further reduction in ΔK_o can be measured in this steel. It is now reasonable to expect why the three structures with identical monotonic yield strengths (i.e., T100, T470, and ISO250) show widely differing values of ΔK_o. The T100 condition has the smallest threshold because this structure is the hardest, due to cyclic hardening. The T470 condition, on the other hand, is the softest condition after cyclic softening, and consequently has the largest threshold.

Fracture morphology of near-threshold fatigue failure consisted of a flat, ductile transgranular mode with isolated segments of intergranular separation (Fig. 10). Close to the threshold, the proportion of intergranular facets was small (< 1%), increasing to a maximum at around ΔK = 6-10 MPa$\sqrt{m}$, and then gradually diminishing at higher stress intensities (Fig. 10b-d). The contribution from intergranular fracture was also found to vary with tempering temperature. Significant amounts of intergranular facets were observed in the T100 and T470 conditions, typically 15% at ΔK = 7 MPa$\sqrt{m}$, compared to a maximum of 8% in the T300 condition, and none at all in the T650 structure.

ii) Effect of Grain Size

To assess the influence of prior austenite grain size on near-threshold fatigue crack growth, specimens were austenitized at 870°C and at 1200°C, oil quenched and tempered at 300°C (referred to as T300 and A1200 structures respectively). The higher austenitizing temperature results in a larger prior austenite grain size (160 μm), yet the strength properties remain largely unaffected. Mechanical properties are listed in Table 2. The fatigue results at R=0.05 and 0.70 (Fig. 11) indicate that growth rates are similar in both structures over the mid-range of growth rates, and begin to differ at high and low stress intensities. At high stress intensities, the A1200 structure shows superior resistance to crack propagation because of increased toughness. At low stress intensities, growth rates are somewhat lower in the coarser-grained A1200 structure, particularly at R=0.05, although the threshold is unchanged. Near-threshold fracture surfaces were much rougher in the coarser structure, showing a facetted, ductile transgranular mode with segments of intergranular fracture.

iii) Effect of Impurity Segregation

The influence of impurity segregation was examined by comparing fatigue crack propagation behaviour in unembrittled and temper embrittled structures. Specimens were austenitized at 870°C, oil quenched and tempered at 650°C. One half of the material was then oil quenched after tempering; the other half was taken through a step-cooling procedure[21] of holding for progressively longer times at decreasing temperatures through the temper embrittlement range. The resulting structures are hereafter referred to as unembrittled (T650) and embrittled (T650SC) respectively. The step-cooling procedure results in a severe loss of toughness (~ 50%) without change in strength (Table 2), concurrent with a change in fracture mode from microvoid coalescence to intergranular. Using Auger spectroscopy, this embrittlement was attributed to the co-segregation of alloying elements (Ni and Mn) and impurity elements (P and Si) to prior austenite grain boundaries.[21]

---

*Cyclic softening in quenched and tempered steels is generally attributed to a rearrangement of dislocation substructure and a reduction in dislocation density with alternating loading. Cyclic hardening has been attributed to dynamic strain ageing, and is characteristic of untempered and lightly tempered steels having high dislocation densities.[36] The lack of softening in the ISO250 condition results from an offsetting effect of transformation-induced hardening of retained austenite to martensite with cyclic strain.[18]

The effect of the impurity segregation on fatigue crack propagation in moist air is shown in Fig. 12 for load ratios of R=0.05 and 0.70. It is clear that prior temper embrittlement results in an increase in crack growth rates at both load ratios, particularly at low stress intensities. At growth rates greater than $\sim 10^{-5}$ mm/cycle, the embrittled structure (T650SC) shows only marginally higher growth rates, and there is little influence of load ratio on crack propagation behaviour in either structure. No major differences were observed in fatigue fracture mechanisms in this region, with both structures exhibiting a transgranular ductile striation mode, similiar to Fig. 5a. At near-threshold growth rates less than 10^{-6} mm/cycle, however, propagation rates in the embrittled structure become over an order of magnitude higher than in the unembrittled structure, and the value of the threshold ΔK_o is significantly reduced from 8.5 to 6.2 MPa$\sqrt{m}$ at R=0.05, and from 3.7 to 2.7 MPa$\sqrt{m}$ at R=0.70. It is also noticable that growth rates are increasingly sensitive to load ratio as the threshold is approached. Significant amounts of intergranular fracture were present in embrittled samples (Fig. 13b); the proportion of which varied with stress intensity. Near ΔK_o the fraction of intergranular fracture was approximately 5%, increasing to around 20% at ΔK = 10 MPa$\sqrt{m}$ (at R=0.05), and then decreasing to zero above ΔK = 15 MPa$\sqrt{m}$. No evidence of intergranular separation could be detected at any stress intensity in unembrittled material (Fig. 13a).

Discussion

The present results have confirmed that microstructure and load ratio effects on fatigue crack propagation in steels occur primarily at high and low growth rates. The mid-range of growth rates, where the crack growth rate curve is linear, has been associated with a ductile striation mechanism of growth, with the exponent 'm' in Eq. (1) found to lie between 2.5 - 2.7. This is consistent with most metallurgical[37] and mechanical models[38-40] of "ductile" fatigue crack growth, which predict an exponent of approximately 2. Such models also predict little influence of load ratio and microstructure on growth rates, and this is clearly verified by the present results in this region. Where the mechanism of failure is by ductile striations, fatigue crack growth appears to be controlled by the amount of crack opening each cycle, dependent upon the elastic modulus.

At high growth rates (regime C), the present results show i) an acceleration in growth rate, ii) increased values of the exponent 'm', iii) large microstructure effects and iv) a marked influence of load ratio. This behaviour has been previously characterised in terms of the occurrence of static fracture modes,[24-26] and such mechanisms have been observed in this region in the present study (Fig. 5). The microstructural influences on growth rate arise here because such static fracture mechanisms are sensitive to material inhomogenities, which control the toughness. An influence of load ratio is observed because cleavage and intergranular cracking are largely tensile stress-controlled fracture modes and fibrous fracture is dependent on the hydrostatic component of stress. Increasing the load ratio raises K_{max} with respect to ΔK, and therefore leads to an increased contribution from such mechanisms. Thus, the onset of an acceleration in growth rate in region C is essentially a function of the toughness, brought about as K_{max} approaches K_{Ic}.

At low growth rates, less the 10^{-6} mm/cycle in region A, fatigue crack growth similarly becomes markedly sensitive to load ratio and microstructure. It is tempting to relate this again to a fracture mechanism change,[24] i.e. the occurrence of intergranular cracking at low values of ΔK (Figs. 10 and 13). However, the lack of such features in the T650 condition (which shows the largest load ratio effect) suggests that this is an oversimplication. It is believed that the occurrence of intergranular cracking in this region is due to the influence of water vapour in air environment, causing hydrogen to diffuse to and embrittle prior austenite grain boundaries, particularly when the plasticity is confined within a single grain. Cooke, et al.[16] have shown that by testing a similar steel *in vacuo* the intergranular fracture largely disappears. Furthermore, the lack of intergranular cracking in the T650 condition is consistent with the fact that this condition is far less sensitive to hydrogen embrittlement.[41] The observation that the overall proportion of grain boundary facets changes with tempering temperature suggests a further influence of the grain boundary strength, which would depend on any impurity segregation there. For example, the largest fraction of intergranular separation during fatigue crack growth can be seen in structures where impurity segregation is likely to have occurred during heat-treatment (ie. T100, T470, and T650SC). All three structures

were observed to fail at least partly by intergranular cracking in monotonic K_{Ic} tests. With T650SC, such fracture was directly identified with the segregation of P and Si (temper embrittlement). For the T100 structure, as-quenched embrittlement is a possibility resulting from the segregation of, say, P in the austenite phase, either prior to, or during quenching after austenitization.[42-44] Finally, the T470 structure involves tempering at a temperature within the tempered martensite embrittlement[45] range for 300-M where impurity separation to grain boundaries is again a strong possibility. There is apparently a close interrelationship here between the sensitivity of the material to the environment (ie. hydrogen embrittlement from moisture in air) and any impurity segregation to grain boundaries, which determines the amount of intergranular separation observed during near-threshold fatigue crack growth in steels. The most significant finding of this study is the dependence of near-threshold fatigue crack propagation rates and the value of the threshold ΔK_o on material strength, since no such dependence has been observed at higher growth rates.[46] Examination of the literature (Fig. 14) indicates that this trend of increasing ΔK_o with decreasing strength clearly exists for steels. Kitagawa, et al[12] and Masounave and Bailon[17] have observed similar effects in much lower strength steels. The present work has shown that such a relationship exists for ultra-high strength steels, provided that cyclic strength is considered rather than the monotonic yield stress. Consequently, cyclic softening must be regarded as beneficial in improving near-threshold crack growth resistance. Coarsening the prior austenite grain size has also been observed to improve near-threshold crack growth resistance although no change in the threshold stress intensity was detected. Results in low strength steels[17] indicate both a decrease in crack growth rate *and* an increase in ΔK_o with larger grain sizes. However, in such steels, there is a reduction in yield strength on coarsening grain size which is not observed in lightly tempered ultra-high strength steels. Finally, the build-up of residual impurities in grain boundaries (temper embrittlement) has been shown to markedly deteriorate crack propagation resistance at near-threshold rates, whereas little effect can be detected at intermediate growth rates.

It is clear from the present results that all the microstructural effects observed principally affect near-threshold fatigue crack propagation behaviour at growth rates less than $\sim 10^{-6}$ mm/cycle, and are far less important at higher propagation rates in the intermediate range. Furthermore, within this regime, growth rates become extremely sensitive to the load ratio, particular in the lower strength conditions (Fig. 9). It is possible to rationalise these results in terms of the influence of the moist air environment on fatigue crack growth. It is generally accepted that the primary mechanism of environmental attack during fatigue crack growth of high strength steels in the presence of water vapour is hydrogen embrittlement.[47] With this in mind, a semi-quantitative model[18,21] is developed relating the contribution to fatigue crack propagation from the environmental effect of hydrogen, evolved from crack tip surface reactions with moist air. This environmental effect can occur under fatigue loading at stress intensities less than the threshold for hydrogen-assisted cracking under monotonic loading (K_{TH} or K_{Iscc}) because fresh surface at the crack tip, where hydrogen can enter the lattice, is continually renewed by cyclic stressing.

Model for Fatigue Crack Growth Threshold in Steels

Following Weiss and Lal,[48] a model for fatigue crack propagation is considered based on the assumption that the crack advance per cycle (da/dN) represents the distance ahead of the crack tip where the nominal stress exceeds a certain critical fracture stress (σ_F), such that

$$\frac{da}{dN} = a\left(\frac{\Delta\sigma_N}{\sigma_F}\right)^{\frac{n_F+1}{n_F}} \cdot f\left(\frac{a}{w}\right) - \rho_*/2 \quad , \qquad \ldots (2)$$

where a is the crack length, $\Delta\sigma_N$ the applied stress amplitude, $f(\frac{a}{w})$ a dimensionless correction factor for the finite width of specimens, n_F the cyclic strain hardening exponent in the stress range to which the critically stressed region is subjected, and ρ_* the Neuber microsupport constant, representing the effective radius of a sharp crack. For near-threshold fatigue crack growth, the maximum cyclic stress

decreases towards the elastic limit, hence n_F must approach unity. Thus, it follows that

$$\frac{da}{dN} = \frac{\Delta K^2}{\pi \sigma_F^2} - \frac{\rho^*}{2} \quad , \qquad \ldots(3)$$

where

$$\Delta K^2 = \pi a \cdot \Delta \sigma_N^2 \cdot f\left(\frac{a}{w}\right) .$$

For crack growth, the local tensile stress (σ_{yy}) must exceed σ_F over a distance larger than ρ^*, and thus, at the threshold, Weiss and Lal[48] suggest $da/dN = \rho^*$, viz.

$$\Delta K_o = \sqrt{\frac{3}{2} \pi \rho^*} \cdot \sigma_F . \qquad \ldots(4)$$

In moist air, however, cyclic stressing will lead to the production of chemically reactive surface at the crack tip, where atomic hydrogen can be evolved from water vapour by reactions[49] of the type

$$Fe + H_2O \rightleftharpoons FeOH^+ + H^+ + 2e$$

$$2H^+ + 2e \rightleftharpoons 2H .$$

The stress gradient ahead of the crack tip then drives adsorbed hydrogen atoms into the lattice where they accumulate in the region of highest dilatation, the point of maximum hydrostatic tension, resulting in a reduction of the cohesive strength.[50] If this reduction in cohesive strength due to hydrogen is taken as $\Delta\sigma_H$, the expression for the threshold in the presence of moist air becomes

$$\Delta K_o = \sqrt{\frac{3}{2} \pi \rho^*} \cdot (\sigma_F - \Delta\sigma_H) . \qquad \ldots(5)$$

Following Oriani and Josephic,[51] it is assumed that $\Delta\sigma_H$ is proportional to the local concentration of hydrogen at the point of highest triaxial tension (C_H), and that this concentration at equilibrium can be obtained from

$$\Delta\sigma_H = \alpha C_H = \alpha C_o \exp \frac{\bar{\sigma} \cdot \bar{V}}{R_o T} , \qquad \ldots(6)$$

where C_o is the equilibrium concentration of hydrogen in the unstressed lattice, α an unknown constant, $\bar{V}$ the partial molar volume of hydrogen in iron (2 cm^3/mole), $\bar{\sigma}$ the hydrostatic tension, R_o the Gas Constant and T the absolute temperature. Combining Eqs. (5) and (6), it follows that

$$\Delta K_o = \sqrt{\frac{3}{2} \pi \rho^*} \cdot \left[\sigma_F - \alpha C_o \exp\left(\frac{\bar{\sigma} \cdot \bar{V}}{R_o T}\right)\right] . \qquad \ldots(7)$$

The hydrostatic tension ($\bar{\sigma}$) is defined as the mean of the three principal stresses ahead of the crack tip (σ_{xx}, σ_{yy}, σ_{zz}), and can be approximated under conditions of plastic flow using Hill's slip-line field equations for plane strain, ie.

$$\bar{\sigma} = \frac{1}{3} (\sigma_{xx} + \sigma_{yy} + \sigma_{zz}) = \alpha_1 \sigma_y \ln\left[\left(1 + \frac{x}{\rho}\right) + \frac{1}{2}\right] , \qquad \ldots(8)$$

where σ_y is the yield strength, x the distance ahead of the crack tip, ρ the crack tip radius and α_1 a coefficient (>1) allowing for an increase in plastic constraint due to work hardening. Rewriting Eq. (8) in terms of the plastic constraint factor ($\sigma_{yy}^{max}/\sigma_y$) ahead of the crack tip,[41] it follows that $\bar{\sigma}$ can be approximated by

$$\bar{\sigma} = \alpha_1 \left(\sigma_{yy}^{max}/\sigma_y - \frac{1}{2}\right) \simeq \sigma_y + 2\alpha_2 K \quad , \qquad \ldots (9)$$

where $\sigma_{yy}^{max}/\sigma_y \simeq 1 + \alpha_2(K/\sigma_y)$.* K is the stress intensity, α_2 an empirical constant = 2 $in^{-1/2}$, and α_1 is taken to be equal to 2. Combining Eqs. (7) and (9) and putting $K = K_{max} = \Delta K/1-R$, where $R = K_{min}/K_{max}$, we have

$$\Delta K_o \simeq \sqrt{\frac{3}{2}\pi\rho_*} \cdot \left\{\sigma_F - \alpha C_o \exp\left[\frac{\bar{V}}{R_o T}\left(\sigma_y + \frac{2\alpha_2 \Delta K_o}{1-R}\right)\right]\right\} \quad \ldots (10)$$

Rearranging Eq. (10), assuming $\frac{\bar{V}\,\alpha_2\,\Delta K_o}{R_o T(1-R)}$ is small, gives

$$\Delta K_o \simeq \sqrt{\frac{3}{2}\pi\rho_*} \cdot \left[\frac{\sigma_F - \alpha C_o \exp(B\sigma_y)}{1 + \dfrac{\alpha C_o \rho_*^{1/2}}{(1-R)} \cdot B' \cdot \exp(B\sigma_y)}\right] , \qquad \ldots (11)$$

where $B = \bar{V}/R_o T$, and $B' = \sqrt{3/2\,\pi} \cdot \bar{V}/R_o T \cdot 2\alpha_2$. At ambient temperature, $B = 8\times10^{-4}$ $(MPa)^{-1}$, and $B' = 5\times10^{-2}$ $(MPa\sqrt{m})^{-1}$.

Evaluation of the remaining parameters in Eq. (11) is complex. The constant α from Eq. (8) is unknown at this time, requiring experimental measurement. Furthermore, the significance of σ_F and ρ_* at the threshold is also uncertain. σ_F represents the critical fracture stress in the absence of environmental influence, and it has been suggested[47] that, at the threshold, this stress approaches the theoretical cohesive strength ($\sigma_c \simeq 1/10$ elastic modulus) acting across a distance ahead of the crack tip of $\rho_* \sim s_o$, where s_o is the cube root of the defect-free volume. For the present steel, assuming average dislocation densities at the crack tip between $10^{12} - 10^{10}/cm^2$, s_o (and hence ρ_*) should be of the order of 100-1000 Å. Finally, the magnitude of C_o will depend on whether the hydrogen is internal (from charging experiments) or external as hydrogen gas or from moisture. For an external gas, C_o is the hydrogen concentration in the unstressed lattice in equilibrium with a hydrogen gas pressure of P_{H_2}, which according to Sievert's Law[51] is given by

$$C_o = \beta\, S_L\, P_{H_2}^{1/2} \quad , \qquad \ldots (12)$$

where S_L is Sievert's parameter for H in α-Fe = 1.26×10^9 atom H/atom Fe $(torr)^{-1/2}$ and β is a multiplicative factor ($\gg 1$), which allows for the fact that the hydrogen solubility in the grain boundaries, where the fractures often occur, may be considerably larger than in the normal lattice. Again the magnitude of C_o remains unclear because of the uncertainty in the value of β. However, the concept of hydrogen-assisted fracture during fatigue crack propagation and the form of Eq. (11) can provide a useful rationalisation of fatigue threshold behaviour in high strength steels. Firstly, any increase in the hydrostatic tension ($\bar{\sigma}$) will markedly increase the local concentration of hydrogen and hence lower the threshold (Eq. 7). This is achieved by i) raising the yield stress and ii) increasing K_{max} or the load ratio R (Eq. 10). Both effects have been experimentally observed in the present investigation (Fig. 9). Furthermore, at high yield strengths, the σ_y term in the

*This expression for the plastic constraint factor was first observed by Hahn and Rosenfield[52] for mild steel, but recent studies[53] have shown that it is also valid for high strength low alloy steels such as 4340.

expression for $\bar{\sigma}$ (Eq. 9) dominates the K_{max} term, suggesting a smaller load ratio effect than at low strengths where the σ_y and K_{max} terms are more comparible. This again is experimentally observed in that the influence of load ratio on ΔK_o increases as the strength decreases (Fig. 9). Moreover, since the effect of load ratio (ie. K_{max}) arises from the environmental contribution, in the absence of an environment (ie. $P_{H_2} \propto C_o = 0$) the value of ΔK_o should be less affected by the load ratio. This is entirely consistent with existing near-threshold data for low-alloy steels,[16] where the influence of load ratio on ΔK_o, measured in air, was found to disappear when tests were performed in a vacuum. Thus, the effect of strength and load ratio on fatigue threshold behaviour in moist air can be thought of in terms of an enhanced environmental influence arising from an increase in the hydrostatic tension. Additionally, increasing the load ratio will raise the magnitude of K_{max} which in turn leads to a larger plastic stress gradient ahead of the crack tip. This provides a greater driving force for the transport of hydrogen into the region of maximum triaxiality. If crack closure effects are considered, however, some influence of load ratio might be expected even *in vacuo*. There is a further possibility that ρ^* may be somewhat related to the yield strength, through changes in the dislocation density, for example. In this instance the value of ΔK_o would be sensitive to material strength in the absence of hydrogen effects. However, data showing the dependence of ΔK_o on yield strength for tests *in vacuo* are not available at this time.

The effect of prior austenite grain size is not so clear. However, it is possible to rationalise the observation of lower growth rates in coarser grained steel in terms of the permeation of hydrogen atoms to grain boundaries. Tien et al.[54] have postulated that the transport of hydrogen atoms from the crack surface into the metal occurs, not by hydrogen diffusion, but through the motion of dislocations ("dislocation sweep-in"). Thus the concentration of hydrogen atoms reaching a grain boundary will be greatest when the maximum plastic zone size is of the order of the grain size.[55] In coarser grained structures the plastic zone size remains small compared to the grain diameter until much higher stress intensities (in the present study $\Delta K \sim 90$ MPa$\sqrt{m}$ in the A1200 structure when maximum plastic zone size equals grain size), resulting in a reduced environmental influence.

Finally, the presence of impurity elements in grain boundaries can be considered to reduce the fracture strength by an amount ($\Delta\sigma_I$), dependent on the reduction ($\Delta\gamma$) in grain boundary surface energy (γ_o) due to the solute,[56] ie.

$$\sigma_F - \Delta\sigma_I \simeq \sigma_c \left(1 - \frac{\Delta\gamma}{\gamma_o}\right)^{1/2} , \qquad \ldots(13)$$

where σ_c is the theoretical cohesive strength. Modification of Eq. (3) to allow for this lowered cohesion due to impurities, ie.

$$\frac{da}{dN} = \frac{\Delta K^2}{\pi(\sigma_F - \Delta\sigma_I)^2} - \frac{\rho^*}{2} , \qquad \ldots(14)$$

predicts higher propagation rates in impurity-embrittled structures at all stress intensities, as has been experimentally shown (Fig. 12). However, at near-threshold growth rates, larger effects of impurity-induced embrittlement are likely due to reduced cohesion from *both* impurities and hydrogen atoms. For example, the presence of an impurity atom in a grain boundary could raise the local hydrogen concentration (C_o), due to an attractive interaction between impurity and hydrogen atoms.[56] Furthermore, there is a possibility that, at chemically active sites (eg. grain boundaries) on freshly exposed surface at the crack tip, where hydrogen is initially adsorbed from the environment, the presence of impurity atoms in embrittled structures could raise the local value of C_o by retarding the recombination of atomic hydrogen.[55] These effects are consistant with the observations that the influence of prior temper embrittlement on fatigue crack growth increases as the propagation rate is decreased (Fig. 12).

It can been seen, therefore, that the influences of microstructure and load ratio observed on near-threshold fatigue crack growth of high strength steels in moist air can be usefully rationalised in terms of a model incorporating the contribution

to crack propagation from the environmental effect of hydrogen. This microstructural and mean stress dependence should, however, disappear at higher (intermediate) growth rates, when hydrogen permeation ahead of the crack tip can no longer keep pace with the crack velocity.* This has been experimental observed for the mid-range of growth rates.

Utilising the model to *quantitatively* predict threshold behaviour requires principally assigning values to two parameters in Eq. (11), namely ρ_*, which has been given some physical significance in terms of the defect-free volume,[48] and (α C_o) which must be fitted empirically. Considering threshold data for steels ranging in strength from 200 to 2000 MPa, best fit was obtained with (α C_o) = 3.5×10^3 MPa. Using this value, with σ_F equated to the theoretical strength, the variation of ΔK_o with yield strength from Eq. (11) is shown by the solid lines in Fig. 14. It can be seen that the experimentally observed trend is correctly reproduced with all threshold values for steels lying within the curves for ρ_* = 300 and 1500 Å, which is reasonable considering the approximate nature of the estimate for $\bar{\sigma}$ (Eq. 9). The values of ρ_* are somewhat large, but still of the same order as those discussed by Weiss and Lal[48] for the threshold range. Further verification of this model must await more extensive data on near-threshold fatigue crack propagation particularly in hydrogen-containing and inert atmospheres.

Conclusions

From a study of fatigue crack propagation in 300-M ultra-high strength steel tested in humid air, the following conclusions can be made:

1. For the mid-range of growth rates (regime B, Fig. 1), variations in microstructure and mean stress (load ratio) do not lead to significant changes in the crack propagation rate. The exponent 'm' in Eq. (1) was found to be between 2.5-2.7, consistent with the ductile striation mechanism of growth observed.

2. At high growth rates (regime C, Fig. 1), crack propagation rates become sensitive to microstructure and load ratio consistent with the occurrence of "static" fracture modes during striation growth. Optimum fatigue cracking resistance in this region is achieved with high toughness materials.

3. At low growth rates (regime A, Fig. 1), significant effects of load ratio and microstructure on the crack propagation rates are observed; the maximum sensitivity to load ratio occurring in lower strength material, and the maximum sensitivity to microstructure occurring at low load ratios.

4. Increased near-threshold crack growth rates and a decrease in the threshold for crack propagation (ΔK_o) are seen as the load ratio (R) is increased, the value of ΔK_o being inversely related to R.

5. Decreased near-threshold crack growth rates are seen as the strength of the steel is reduced, the value of ΔK_o being inversely related to the cyclic yield strength. Cyclic softening (and the use of low strength steels) can thus be regarded as beneficial in improving resistance to very high cycle, low growth rate ($< 10^{-6}$ mm/cycle) fatigue crack propagation.

6. Decreased near-threshold crack growth rates are seen as the prior austenite grain size is increased, the value of ΔK_o remaining unchanged. Thus coarsening the microstructure appears beneficial to near-threshold crack propagation resistance.

7. Increased near-threshold crack growth rates and significantly lower thresholds are observed in steel previously subjected to impurity-induced embrittlement during heat-treatment.

8. A model for the threshold (ΔK_o) for fatigue crack propagation in steels in the presence of a moist air environment is developed based on a critical stress criterion for growth modified by the effect of hydrogen from the environment. The model is seen to rationalise the experimentally observed trends of microstructure and load ratio on near-threshold growth rates and the value of ΔK_o.

---

*Microstructural and load ratio effects can re-appear at higher crack propagation rates, due to the occurrence of static modes of fracture during striation growth.

Acknowledgements

The research was conducted under the auspices of the U.S. Energy Research and Development Administration through the Materials and Molecular Division of the Lawrence Berkeley Laboratory. The author acknowledges the Miller Institute for Basic Research in Science for the award of a University Miller Research Fellowship, and Professors E. R. Parker and V. F. Zackay for their support and encouragement.

References

1. I. Gray, M. Heaton and G. Oates, Proceedings of British Steel Corporation Conf. on "Mechanics and Mechanisms of Crack Growth," Cambridge, April, 1973, p.264. (British Steel Corporation, Special Steels Div., Rotherham 1974).
2. M. Heaton, Proceedings of Institute of Physics/Metals Society Conf. on "Mechanics and Physics of Fracture," Cambridge, Jan. 1975, p. 4/1.
3. H. H. Johnson and P. C. Paris, Eng. Fracture Mech., 1968, 1, 3.
4. P. C. Paris and F. Erdogan, J. Basic Eng. (Trans. ASME [D]), 1963, 85, 528.
5. N. E. Frost, L. P. Pook and K. Denton, Eng. Fracture Mech., 1971, 3, 109.
6. M. Klesnil and P. Lukáš, ibid., 1972, 4, 77.
7. M. Klesnil and P. Lukáš, Mater. Sci. Eng., 1972, 9, 231.
8. L. P. Pook, A.S.T.M. Spec. Tech. Publ., (513), p.106, 1972.
9. R. J. Bucci, P. C. Paris, R. W. Hertzberg, R. A. Schmidt and A. F. Anderson, ibid., p. 125.
10. P. C. Paris, R. J. Bucci, E. T. Wessel, W. G. Clark and T. R. Mager, ibid., p. 141.
11. R. J. Bucci, W. G. Clark and P. C. Paris, ibid., p. 177.
12. H. Kitagawa, H. Nishitani and J. Matsumoto, Proceedings 3rd Int. Congress on Fracture, Munich, 1973, Paper V-444/A.
13. R. A. Schmidt and P. C. Paris, A.S.T.M Spec. Tech. Publ. (536), p. 79, 1973.
14. J. L. Robinson and C. J. Beevers, Metal Sci. J., 1973, 7, 153.
15. P. E. Irving and C. J. Beevers, Metall. Trans., 1974, 5, 391.
16. R. J. Cooke, P. E. Irving, G. S. Booth and C. J. Beevers, Eng. Fracture Mech., 1975, 7, 69.
17. J. Masounave and J-P. Baïlon, Scripta Met., 1976, 10, 165.
18. R. O. Ritchie, J. Eng. Mats. and Tech., (Trans. ASME [H]), 1977, in press. (Lawrence Berkeley Laboratory Report LBL-5496, Oct. 1976).
19. A. J. McEvily and J. Groeger, Proceedings 4th Int. Conf. on Fracture, Waterloo, Canada, June 1977.
20. R. O. Ritchie, ibid. (Lawrence Berkeley Laboratory Report No. LBL-5188, June 1976).
21. R. O. Ritchie, Metall. Trans. A, 1977, in press (Lawrence Berkeley Laboratory Report No. 5498, Oct. 1976).
22. C. Laird and G. C. Smith, Phil. Mag., 1962, 7, 847.
23. R. M. N. Pelloux, Eng. Fracture Mech., 1970, 1, 697.
24. C. E. Richards and T. C. Lindley, ibid., 1972, 4, 951.
25. R. O. Ritchie and J. F. Knott, Acta Met., 1973, 21, 639.
26. R. O. Ritchie and J. F. Knott, Mater. Sci. Eng., 1974, 14, 7.
27. J. A. Feeney, J. C. McMillan and R. P. Wei, Metall. Trans., 1970, 1, 1741.
28. W. Elber, A.S.T.M. Spec. Tech. Publ. (486), p. 230, 1971.
29. T. C. Lindley and C. E. Richards, Mater. Sci. Eng., 1976, 14, 281.
30. F. J. Pitaniak, A. F. Grandt, L. T. Montulli and P. F. Packman, Eng. Fracture Mech., 1974, 6, 663.
31. P. E. Irving, J. L. Robinson and C. J. Beevers, Int. J. Fract., 1973, 9, 105.
32. O. Buck, J. D. Frandsen and H. L. Marcus, Eng. Fracture Mech., 1975, 7, 167.
33. P. E. Irving, J. L. Robinson and C. J. Beevers, ibid., 1975, 7, 619.
34. T. T. Shih and R. P. Wei, ibid., 1974, 6, 19.
35. R. O. Ritchie, G. G. Garrett and J. F. Knott, Int. J. Fract. Mech., 1971, 7, 462.
36. P. N. Thielen, M. F. Fine and R. A. Fournelle, Acta. Met., 1976, 24, 1.
37. R. M. N. Pelloux, Eng. Fracture Mech., 1970, 1, 697.
38. H. W. Liu, J. Basic Eng., (Trans ASME [D]), 1963, 85, 116.
39. S. D. Antolovich, A. Saxena and G. R. Chanani, Eng. Fracture Mech., 1975, 7, 649.
40. S. Purushothaman and J. K. Tien, Scripta Met., 1975, 9, 923.
41. W. W. Gerberich and Y. T. Chen, Metall. Trans. A, 1975, 6A, 271.
42. B. J. Schulz and C. J. McMahon, Jr., A.S.T.M. Spec. Tech. Publ., (499), p.104, 1972.

43. G. Clark, R. O. Ritchie and J. F. Knott, Nature Phys. Sci., 1972, 239, 104.
44. H. Ohtani and C. J. McMahon, Jr., Acta Met., 1975, 23, 377.
45. J. M. Capus, Rev. Met., 1959, 56, 181.
46. J. Barsom, E. J. Imhof and S. T. Rolfe, Eng. Fracture Mech., 1970, 2, 301.
47. R. P. Wei and J. D. Landes, Mats. Res. Standards, 1969, 9, 25.
48. V. Weiss and D. N. Lal, Metall. Trans., 1974, 5, 1946.
49. T. Misawa, Corrosion Sci., 1973, 13, 659.
50. A. R. Troiano, Trans. ASM, 1960, 52, 54.
51. R. A. Oriani and P. H. Josephic, Acta Met., 1974, 22, 1065.
52. G. T. Hahn and A. R. Rosenfield, Trans. ASM, 1966, 59, 909.
53. A. T. Santhanam, Proc. 2nd Int. Conf. on Mech. Behaviour of Materials, Boston, Aug. 1976, p. 1022.
54. J. K. Tien, R. J. Richards, O. Buck and H. L. Marcus, Scripta Met., 1975, 9, 1097.
55. J. D. Frandsen and H. L. Marcus, "Effect of Hydrogen on Behaviour of Materials" (ed. A. W. Thompson and I. M. Bernstein), 1975, p. 233. (The Metallurgical Society of AIME, 1975).
56. C. J. McMahon, Jr., C. L. Briant and S. K. Banerji, Proceedings of 4th Int. Conf. on Fracture, Waterloo, Canada, June 1977.

Tables

Table 1. Composition in wt% of aircraft-quality (vacuum-arc remelted) 300-M low alloy steel.

C	Mn	Cr	Ni	Mo	Si	S	P	V
0.42	0.76	0.76	1.76	0.41	1.59	0.002	0.007	0.10

Table 2. Ambient temperature mechanical properties of 300-M steel.

Code	0.2% Offset Yield Stress		U.T.S.	Elongation	K_{Ic}	Prior Austenite Grain Size
	Monotonic	Cyclic				
	(MPa)	(MPa)	(MPa)	(% of 1 in. gauge)	(MPa$\sqrt{m}$)	(μm)
T100	1497	2107	2338	12.4	35.5	20
T300	1737	1486	2006	11.9	65.1	20
T470	1497	1198	1683	12.1	68.9	20
T650	1074	861	1186	18.1	185[1] 152[2]	20
T650SC	1070	858	1179	14.9	79.6	20
ISO250	1497	1502	1862	14.5	88.5	20
A1200	1657	1571	1986	6.3	80.3	160

[1]Invalid K_{Ic} result, estimated using equivalent energy procedure at maximum load.[21]
[2]Invalid K_{Ic} result, estimated using J_{Ic} procedure at crack initiation.[21]

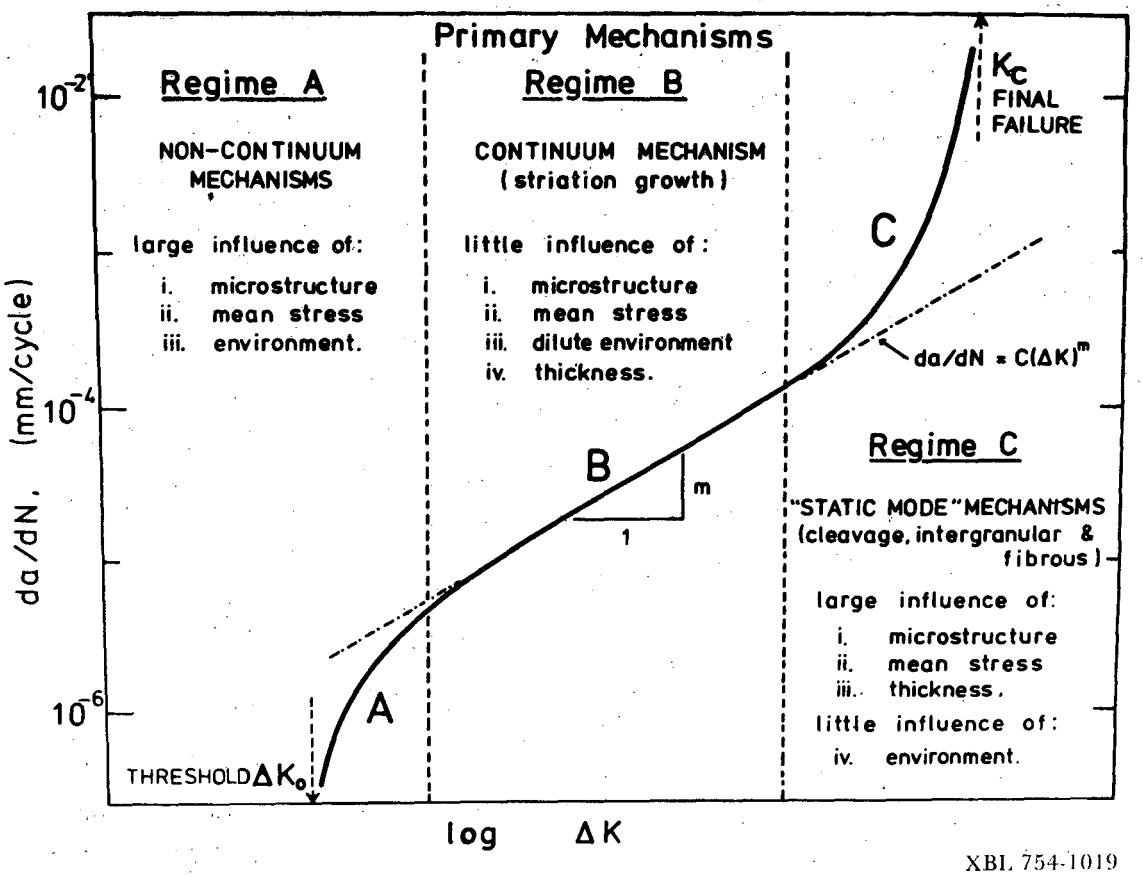

Fig. 1. Showing the primary fracture mechanisms in steels associated with the sigmoidal variation of fatigue crack propagation rate (da/dN) with alternating stress intensity (ΔK).

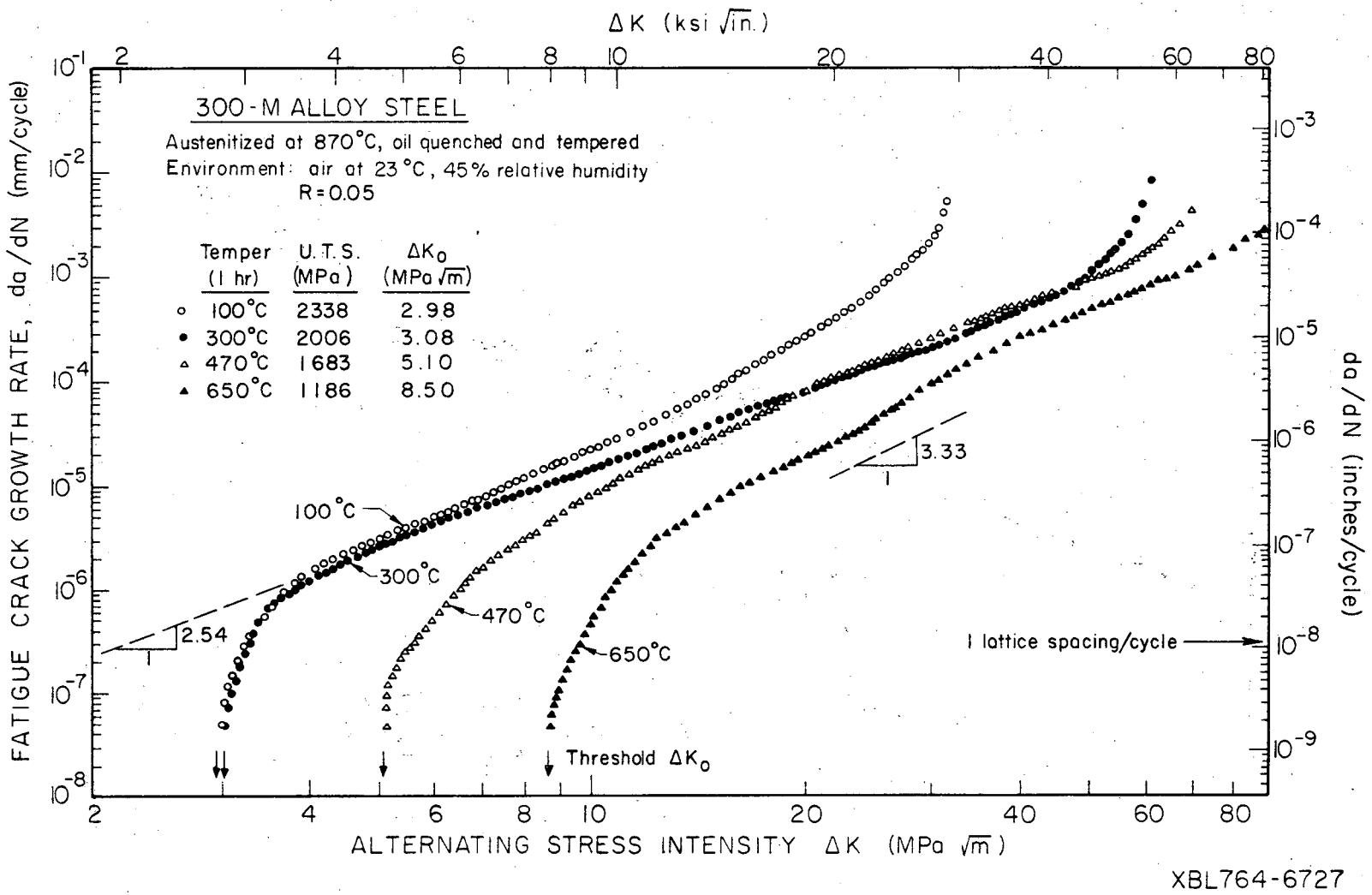

Fig. 2. Fatigue crack propagation results for 300-M, quenched and tempered between 100°C and 650°C, showing influence of material strength at R=0.05.

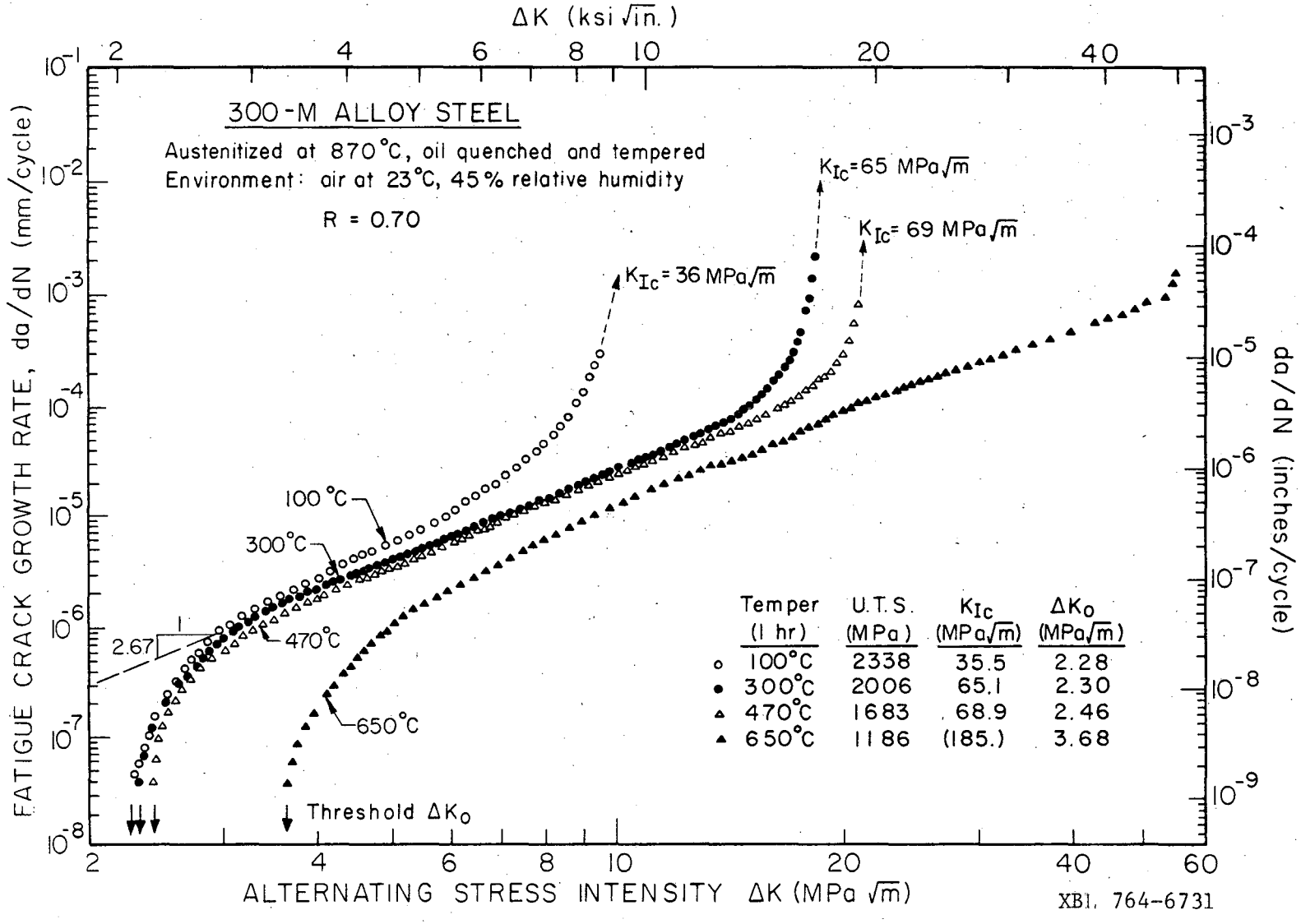

Fig. 3. Fatigue crack propagation results for 300-M, quenched and tempered between 100°C and 650°C, showing influence of material strength at R=0.70.

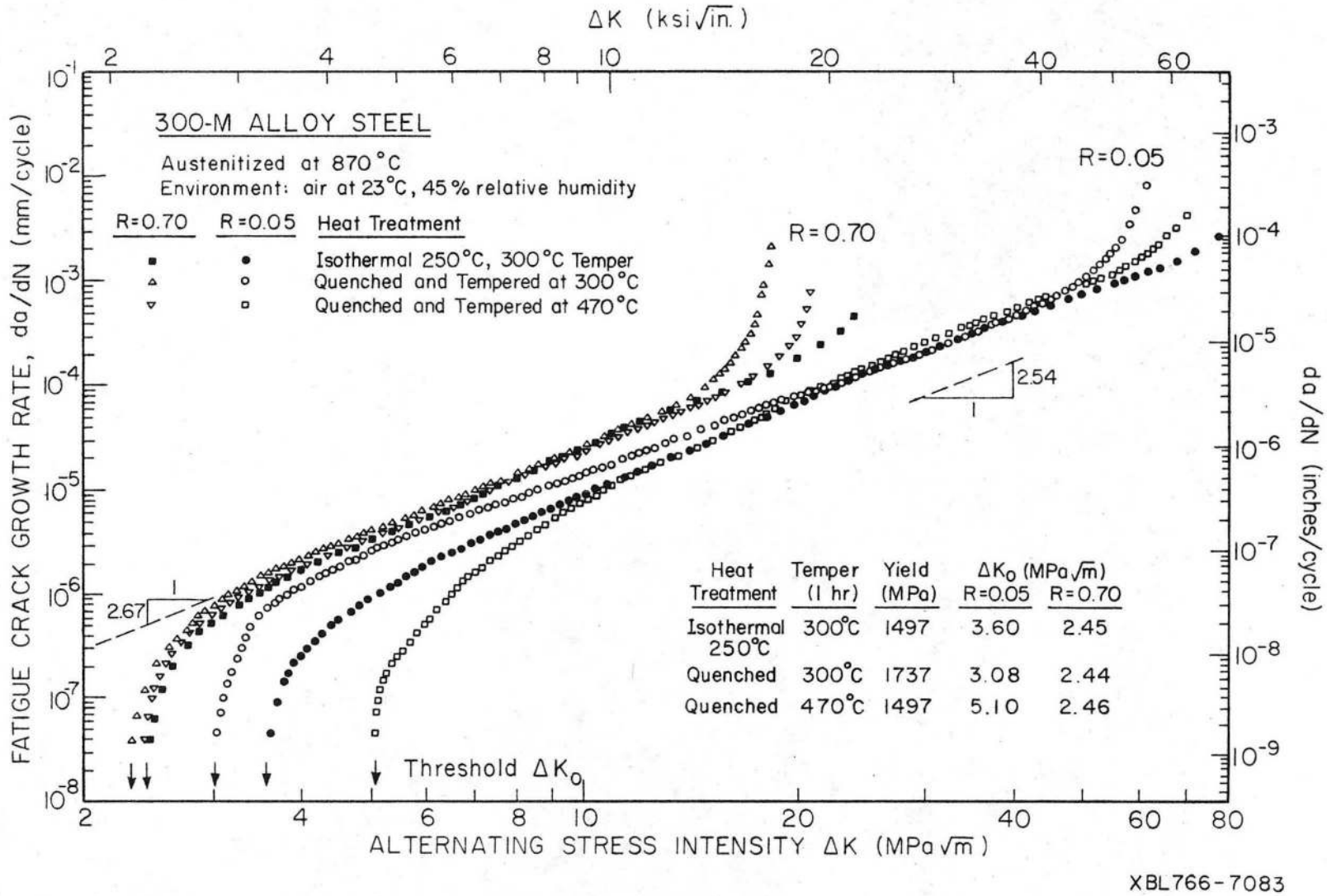

XBL766-7083

Fig. 4. Fatigue crack propagation results for 300-M, isothermally transformed at 250°C (IS0250), compared with T300 and T470 structures at R=0.05 and 0.70.

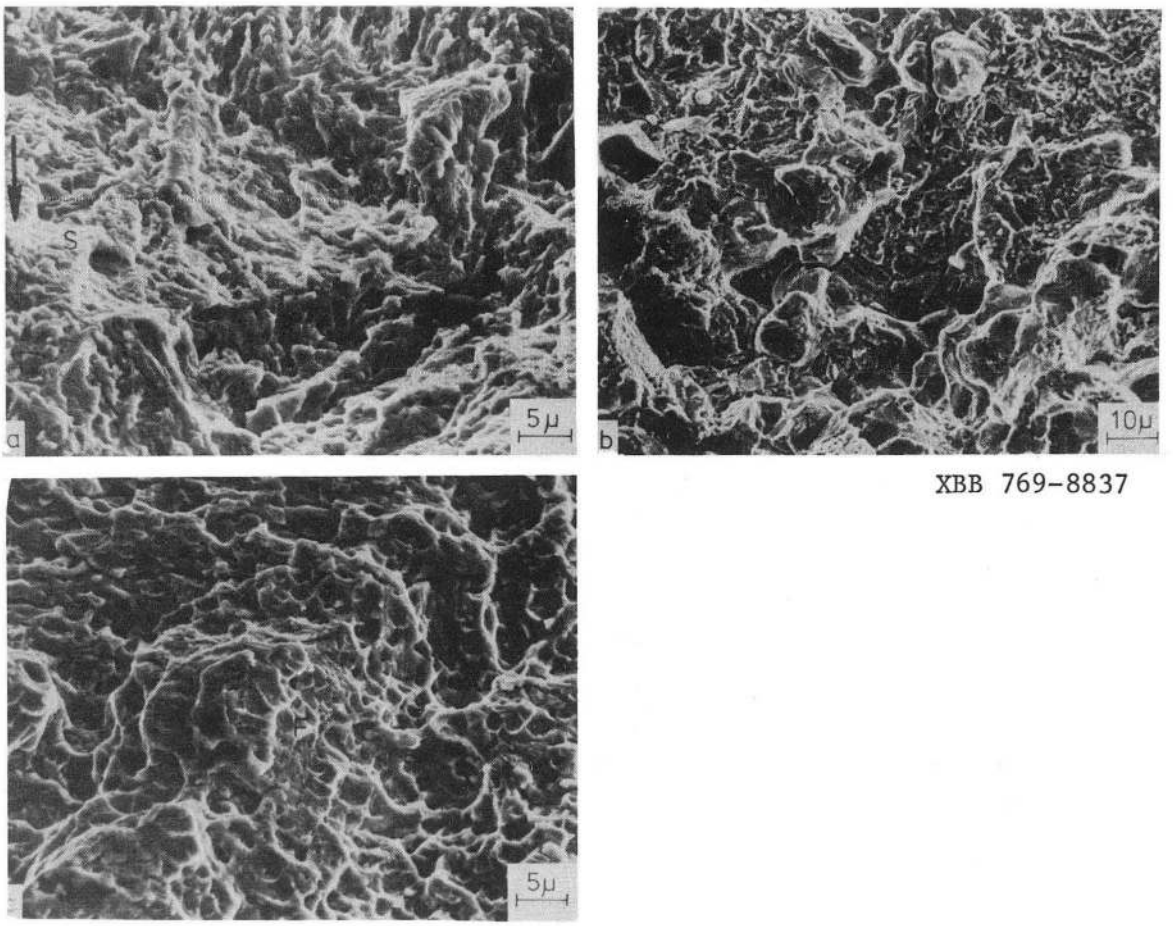

XBB 769-8837

Fig. 5. Mechanisms of growth at medium and high growth rates (R=0.05). a) Ductile striation growth in T300 condition at ΔK = 20 MPa$\sqrt{m}$; b) Intergranular, cleavage and fibrous fracture at high growth rates in T100 condition at ΔK = 30 MPa$\sqrt{m}$; and c) fibrous fracture in T300 condition at ΔK = 60 MPa$\sqrt{m}$. [Arrow indicates general direction of crack propagation.]

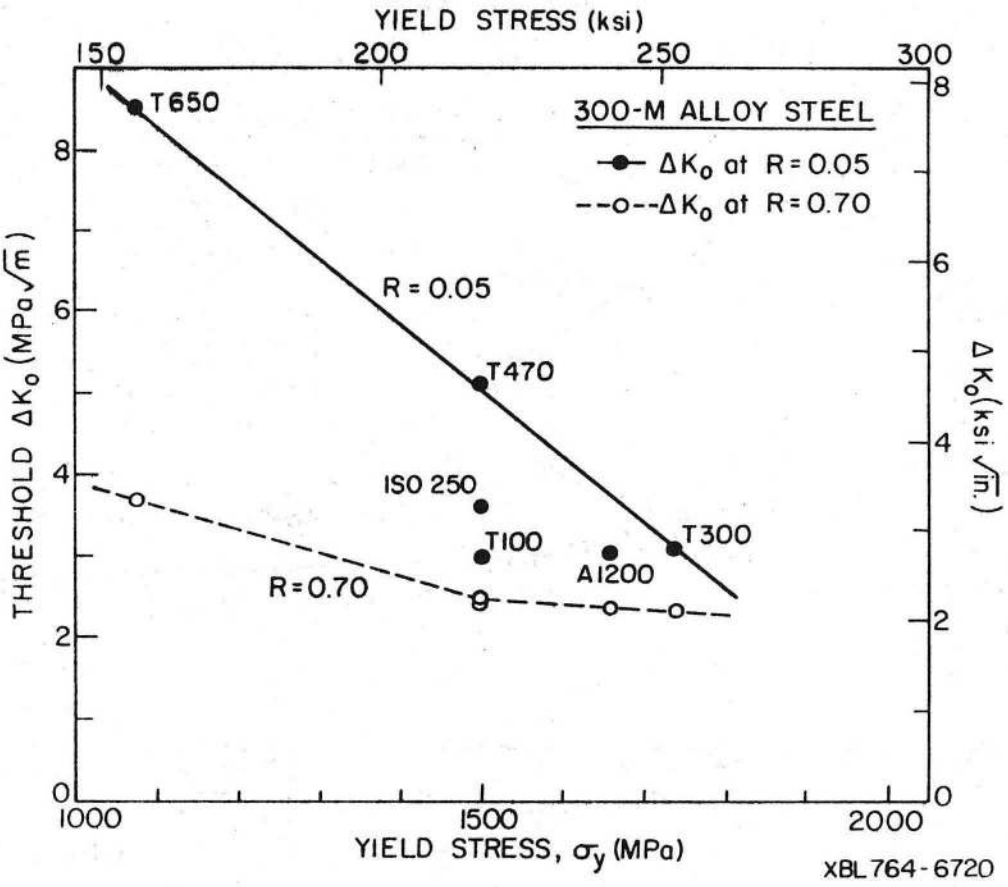

Fig. 6. Influence of monotonic yield strength (σ_y) on threshold for fatigue crack growth (ΔK_o).

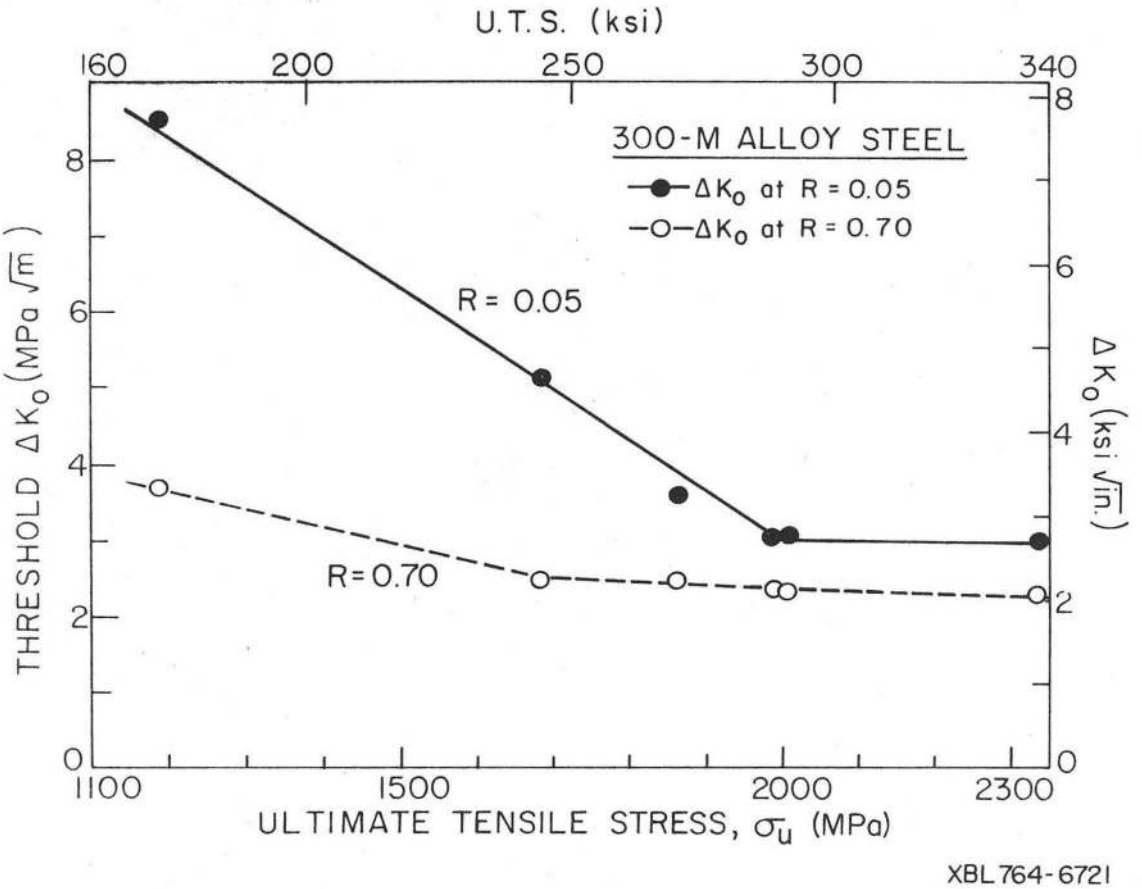

Fig. 7. Influence of ultimate tensile strength (U.T.S.) on threshold for fatigue crack growth (ΔK_o).

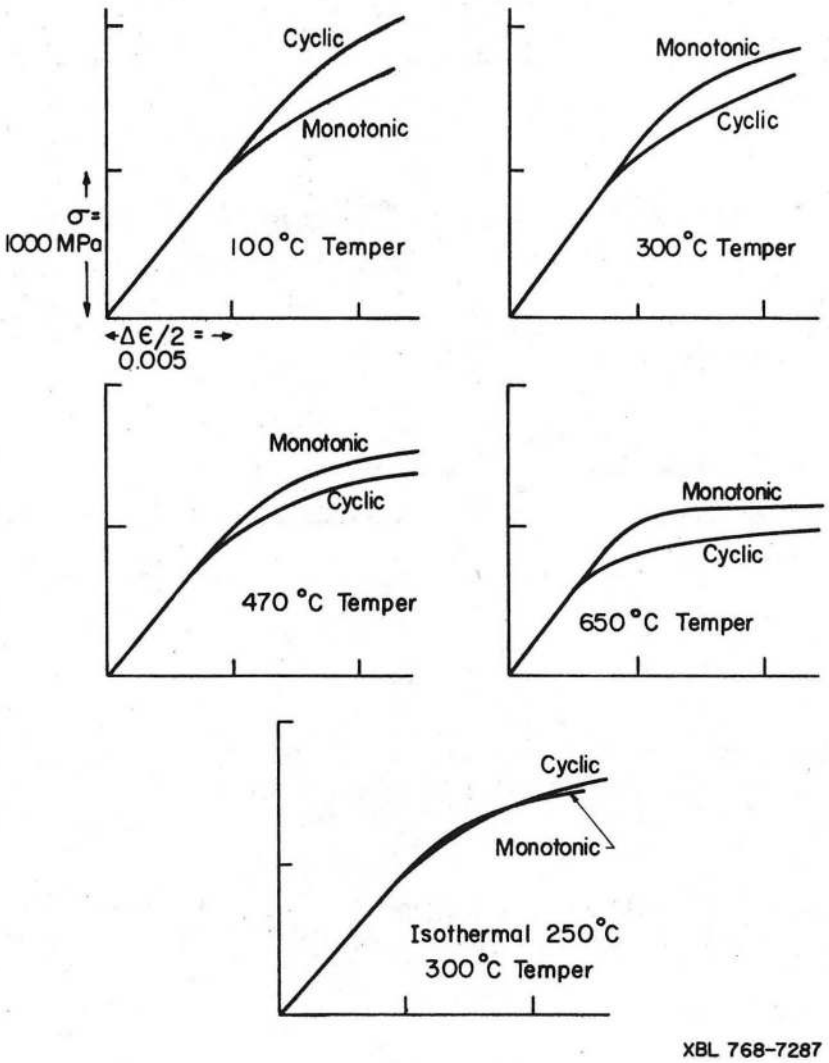

Fig. 8. Monotonic and cyclic stress-strain curves for 300-M steel.

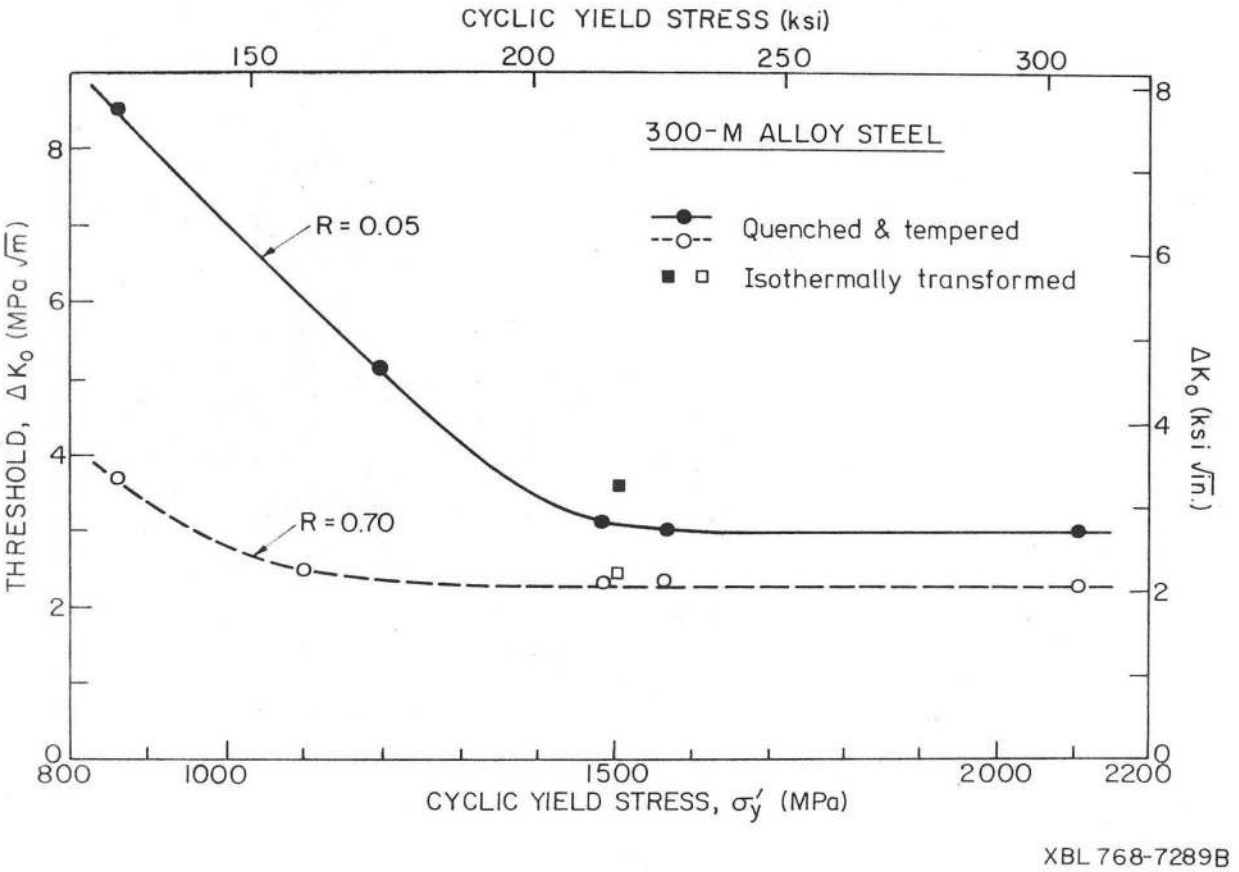

Fig. 9. Influence of cyclic yidld strength ($\sigma_{y'}$), measured by 0.2% offset, on threshold for fatigue crack growth (ΔK_o).

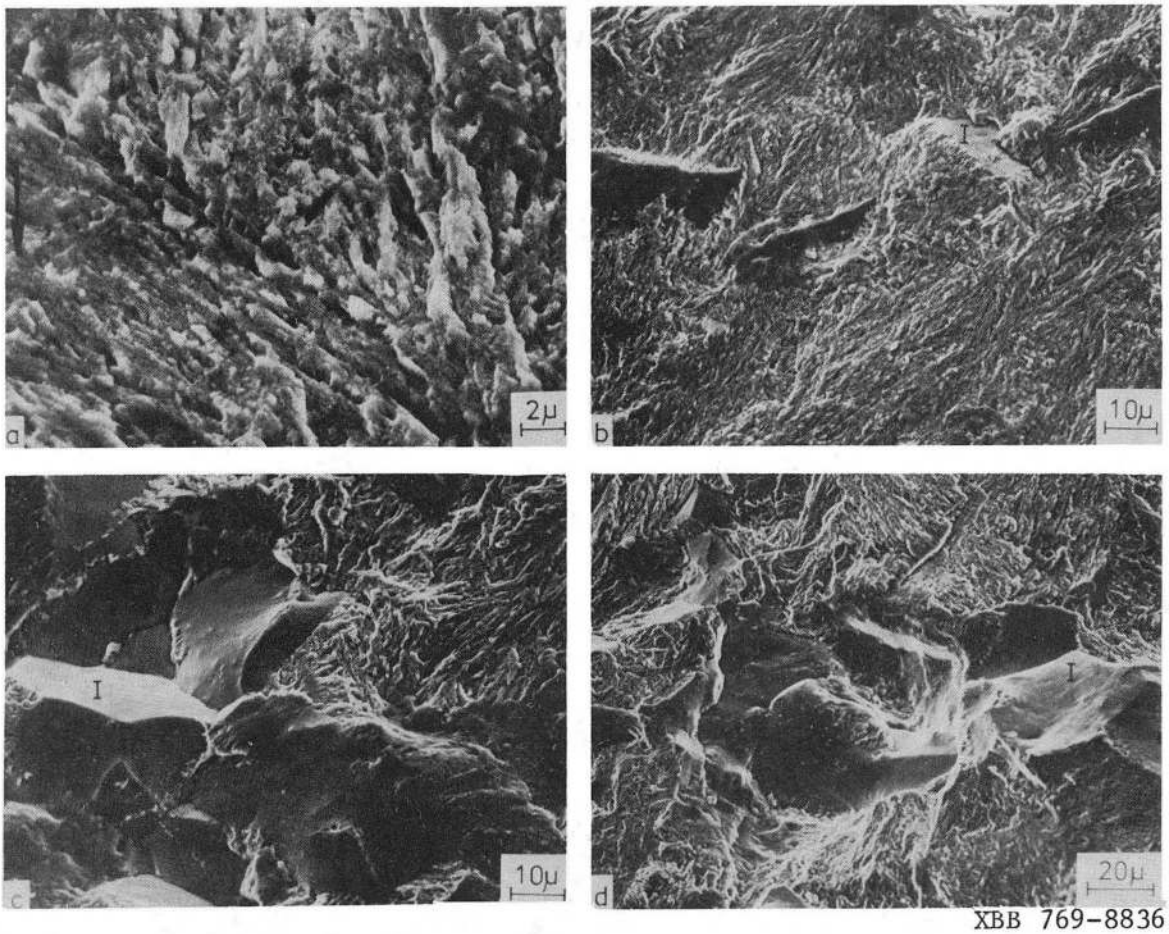

XBB 769-8836

Fig. 10. Mechanisms of growth at low growth rates, showing ductile transgranular mechanism with segments of intergranular fracture (I), in T470 condition at R=0.5. a) & b) At threshold, ΔK = 5.2 MPa$\sqrt{m}$, c) ΔK = 7.6 MPa$\sqrt{m}$, and d) ΔK = 11 MPa$\sqrt{m}$.

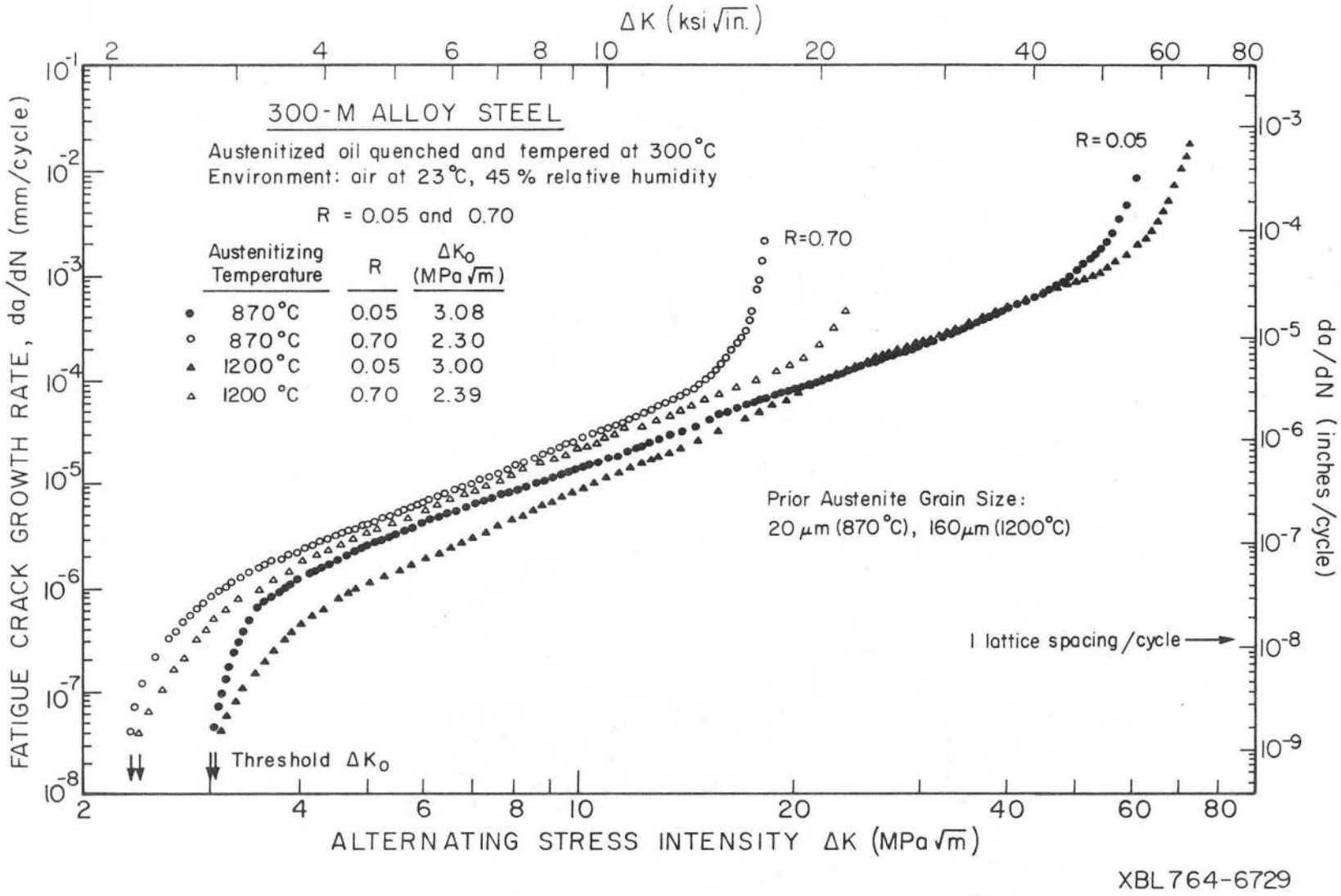

Fig. 11. Fatigue crack propagation results for 300-M, austenitized at 870°C (T300) and at 1200°C (A1200), showing influence of grain size.

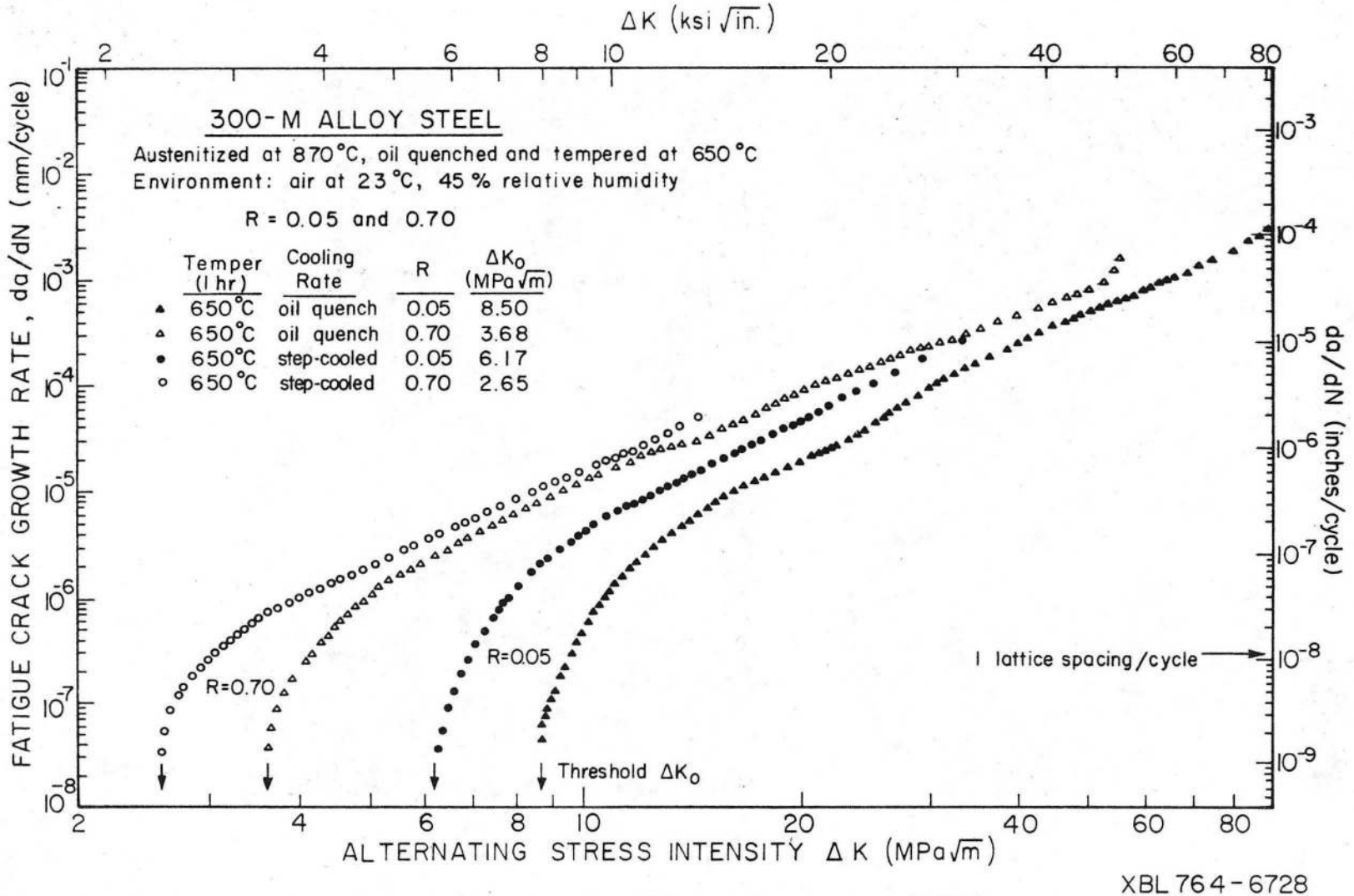

Fig. 12. Fatigue crack propagation results for 300-M, oil quenched (T650) and step-cooled (T650SC) after tempering at 650°C, showing influence of impurity-induced embrittlement.

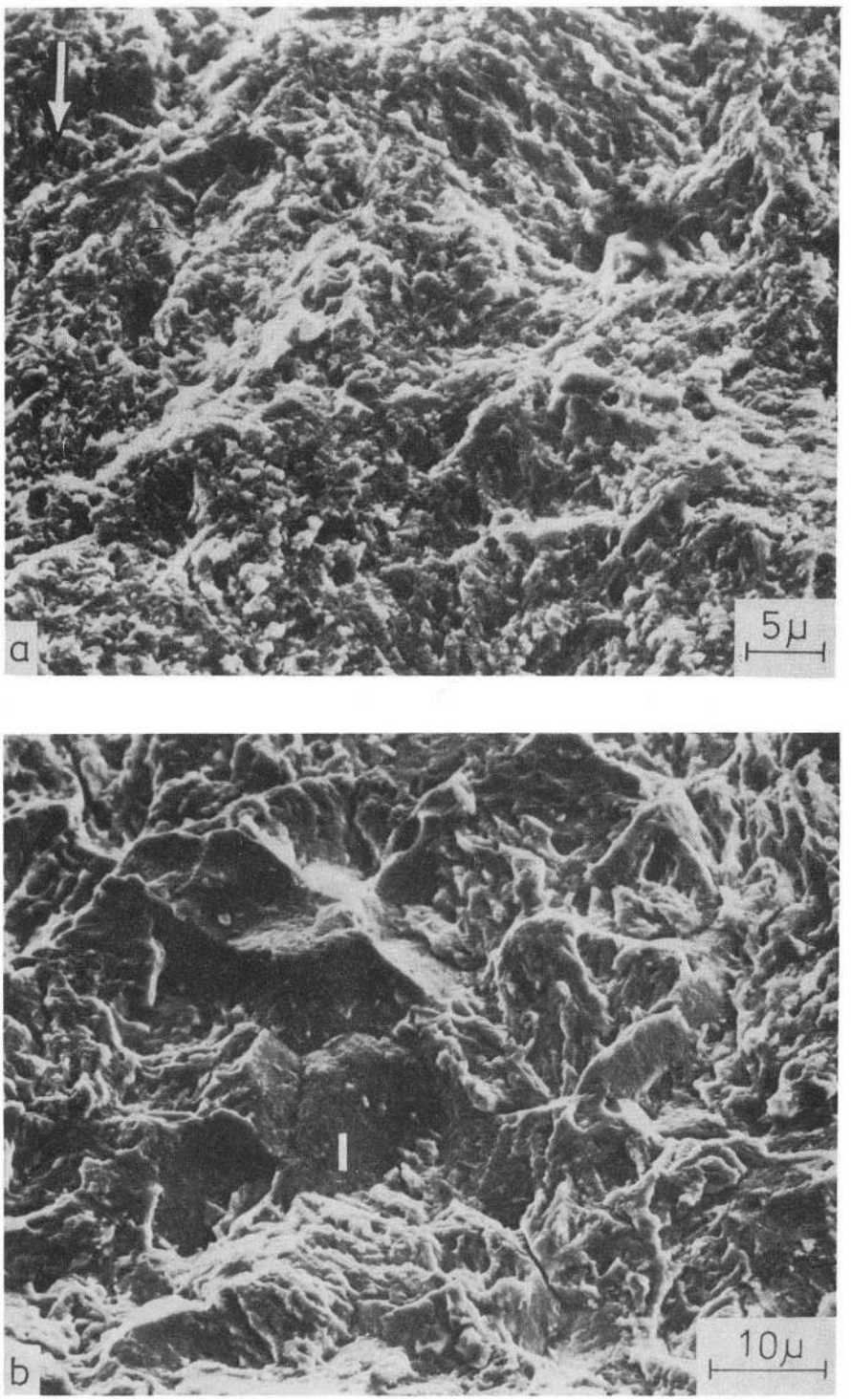

XBB 764-3784

Fig. 13. Morphology of fatigue fracture at near-threshold crack growth rates at $\Delta K = 9.5$ MPa$\sqrt{m}$ (R=0.05) in 300-M steel showing a) ductile transgranular mechanism in unembrittled material (T650), and b) segments of intergranular mechanism in unembrittled material (T650), and b) segments of intergranular fracture (I) in temper embrittled material (T650SC).

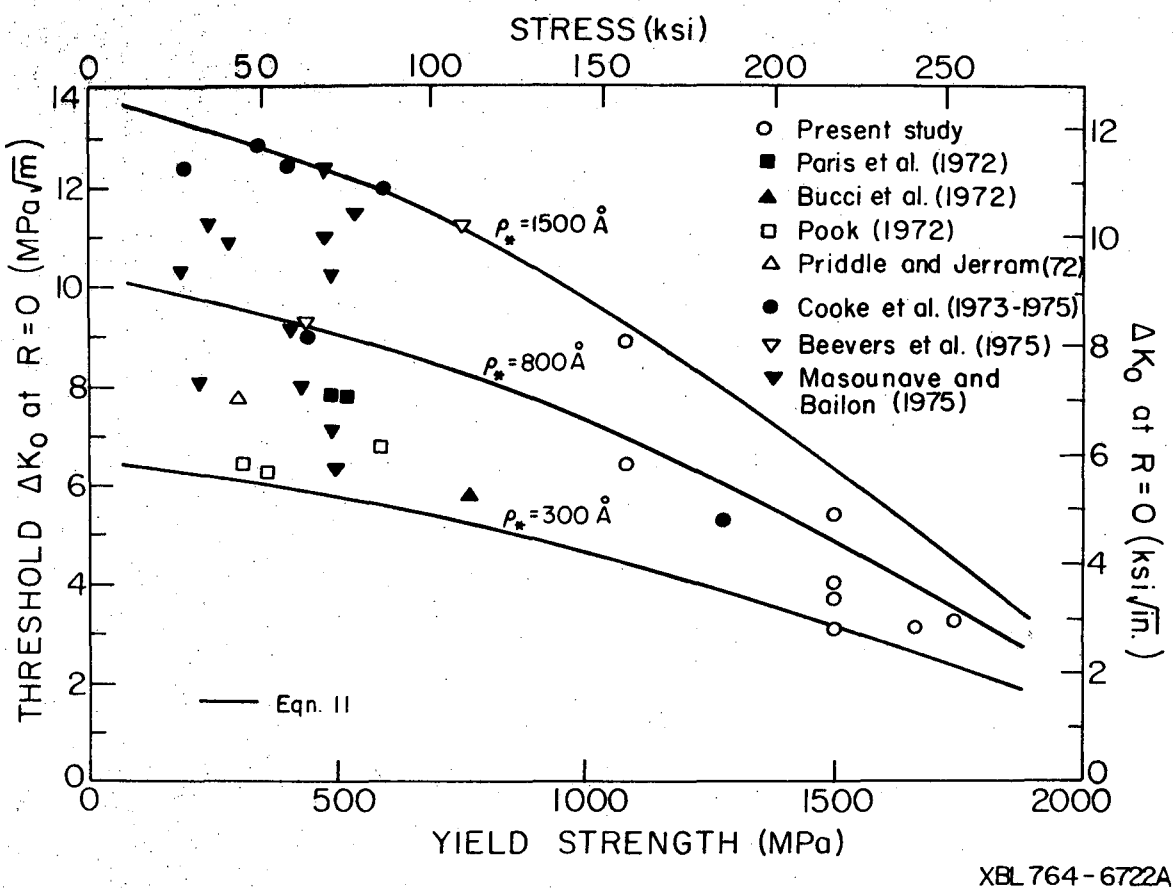

Fig. 14. Summary of results showing variation of thershold for fatigue crack growth (ΔK_o) at R=0 with yield strength for steels. Solid lines from thershold model (Eq. 11).

TECHNICAL INFORMATION DIVISION
LAWRENCE BERKELEY LABORATORY
UNIVERSITY OF CALIFORNIA
BERKELEY, CALIFORNIA 94720